



ELSEVIER

Contents lists available at ScienceDirect

Plant Physiology and Biochemistry

journal homepage: www.elsevier.com/locate/plaphy

Research article

The selenium-binding protein of *Theobroma cacao*: A thermostable protein involved in the witches' broom disease resistance

Akyla Maria Martins Alves^a, Sara Pereira Menezes^a, Eline Matos Lima^a, Karina Peres Gramacho^b, Bruno Silva Andrade^c, Monaliza Macêdo Ferreira^a, Carlos Priminho Pirovani^a, Fabienne Micheli^{a,d,*}

^a Universidade Estadual de Santa Cruz (UESC), Departamento de Ciências Biológicas (DCB), Centro de Biotecnologia e Genética (CBG), Rodovia Ilhéus-Itabuna, km 16, 45662-900, Ilhéus-BA, Brazil

^b Cocoa Research Center, CEPLAC/CEPEC, 45600-970, Itabuna-BA, Brazil

^c Universidade Estadual do Sudoeste da Bahia (UESB), Av. José Moreira Sobrinho, Jequié, Bahia, 45206-190, Brazil

^d CIRAD, UMR AGAP, F-34398, Montpellier, France

ARTICLE INFO

Keywords:

Moniliophthora perniciosa

Selenium

Molecular docking

Gene expression

ABSTRACT

The selenium-binding proteins are known to be inducers of apoptosis in human and animals, and have been studied as target for the treatment of various types of cancer. In plants, SBP expression has been related to abiotic and biotic stress resistance. The SBP from *Theobroma cacao* (TcSBP) was first identified from a cocoa-*Moniliophthora perniciosa* cDNA library. The present study provides details on the TcSBP gene and protein structure. Multiple alignments revealed conserved domains between SBP from plants, human and archae. Homology modeling and molecular docking were performed and showed that the TcSBP has affinity to selenite in the active CSSC site. This result was confirmed by circular dichroism of the recombinant TcSBP, which also presented thermostable behavior. RT-qPCR analysis showed that TcSBP was differentially expressed in resistant vs susceptible cacao varieties inoculated by *M. perniciosa* and its expression was probably due to hormone induction via cis-regulating elements present in its promotor. The presence of the CSSC domain suggested that TcSBP acted by altering oxidation/reduction of proteins during H₂O₂ production and programmed cell death in the final stages of the witches' broom disease. To our knowledge, this is the first *in silico* and *in vitro* analysis of the SBP from cacao.

1. Introduction

Cacao is an endemic plant of tropical forests in South America and is grown mainly for the production of cocoa liquor, butter and powder for the chocolate industry (Wood and Lass, 1985). However, cocoa production has been severely damaged by diseases caused by fungi and oomycetes (Evans, 2007). In Brazil, the witches' broom disease caused by the basidiomycete *Moniliophthora perniciosa* caused drastic economic and social changes in the affected areas (Evans, 2007). *Moniliophthora perniciosa* has two distinct phases of development: a biotrophic phase characterized by a monokaryotic and intercellular mycelium, and a necrotrophic phase characterized by a dikaryotic and intracellular mycelium (Ceita et al., 2007; Sena et al., 2014). The transition from biotrophic to necrotrophic phase is characterized by significant accumulation of H₂O₂ and by programmed cell death (PCD). In cacao plants susceptible to *M. perniciosa*, the PCD occurs initially as a defense

mechanism and then is deflected by the fungus for its own profit, allowing sporulation and further propagation (Ceita et al., 2007). Thus, the study of compounds, genes and proteins that induce PCD and/or facilitate the transition from biotrophic to necrotrophic phase (Ceita et al., 2007; Sena et al., 2014) is important to better understand the cacao-*M. perniciosa* pathosystem and to develop strategies for witches' broom disease control.

The selenium-binding protein (SBP) is known as a tumor suppressor involved in the regulation of cell proliferation, senescence, migration and apoptosis (Zhang et al., 2013) and has been studied as a target for the treatment of various types of cancer in animals and human, generally in related studies (Ansong et al., 2014). In human, it has been reported that the expression of the SBP gene was reduced in tumor tissues when compared to healthy ones, and for this reason, this gene has been indicated as a good predictor of clinical outcome of cancer (Zhang et al., 2013). SBP was also related to resistance to abiotic and

* Corresponding author. UESC, DCB, Rodovia Ilhéus-Itabuna km16, 45662-900, Ilhéus-BA, Brazil.

E-mail address: fabienne.micheli@cirad.fr (F. Micheli).

<https://doi.org/10.1016/j.plaphy.2019.08.005>

Received 24 January 2019; Received in revised form 23 June 2019; Accepted 8 August 2019

Available online 10 August 2019

0981-9428/ © 2019 Elsevier Masson SAS. All rights reserved.

biotic stresses in plants (Sawada et al., 2004; Agalou et al., 2005). In several plant species, studies showed the correlation between SBP level and tolerance to metal toxicity (e.g. by Se/selenite SeO_3^{2-} , cadmium and sulfur) suggesting that SBP participated to metal detoxification mechanism (Agalou et al., 2005). In Arabidopsis, SBP1 was considered a general stress-responsive gene (Valassakis et al., 2018). In transgenic rice plants (*Oryza sativa*), the overexpression of *OsSBP* increased the plant resistance to the rice blast disease caused by the fungus *Pyricularia grisea*, and to the bacterial blight due to *Xanthomonas oryzae* pv. *oryzae* (Sawada et al., 2003, 2004). The SBP function was related to its ability to bind Se covalently (Zhang et al., 2013) and to the regulation of Se and SeO_3^{2-} metabolism (Zhang et al., 2013).

The selenium-binding protein gene from *Theobroma cacao* (*TcSBP*) was first identified from a cocoa-*Moniliophthora perniciosa* cDNA library (Gesteira et al., 2007). Here, we identified and analyzed *in silico* and *in vitro* the unique SBP sequence found in the *T. cacao* genome. The aim of this study was to understand the role of *TcSBP* during the cocoa-*M. perniciosa* interaction as well as to identify possible action mechanisms of this protein associated to its ligation to selenite.

2. Methods

2.1. *In silico* analysis of *TcSBP*

The *TcSBP* cDNA was identified from a library of *T. cacao* meristem (genotype TSH1188) infected by *M. perniciosa* (Gesteira et al., 2007). The complete sequence of the entire gene and of the corresponding proteins was obtained from the CocoaGenDB database (<http://cocoa-genome-hub.southgreen.fr/>). Open reading frame (ORF) detection was performed using the ORFinder software (<http://www.ncbi.nlm.nih.gov/gorf/gorf.html>). Sequence homology search was made with BLAST (Altschul et al., 1997) on the National Center for Biotechnology Information (NCBI). Multiple sequence alignment was performed with the ClustalW2 software (Larkin et al., 2007). The prediction of theoretical isoelectric point (pI) and molecular weight (MW) was obtained using the ProtParam tool (<https://web.expasy.org/protparam/> (Gasteiger et al., 2005)). Post-translational events were predicted using the NetPhos 2.0 Server to identify putative sites of phosphorylation (Ser/Thr/Tyr) (Blom et al., 1999) and NetNGlyc 1.0 Server (<http://www.cbs.dtu.dk/services/NetNGlyc/>) to identify putative sites of N-glycosylation. Predictions of subcellular localization were conducted with the programs TargetP 1.1 server (Emanuelsson et al., 2007) and PSORT (Nakai and Horton, 1999). Signal peptide presence was analyzed using the SignalP 4.0 Server (Petersen et al., 2011). The *TcSBP* was used, together with the sequences of the homolog proteins from other plants and mammals, to construct an unrooted phylogenetic tree by the neighbor joining method with the ClustalW2 (Larkin et al., 2007) and MEGA 6 (Tamura et al., 2013) programs. For the dendrogram analysis, only complete sequences with high identity (> 70%) from plants and mammals were considered. The tree was constructed using the neighbor-joining method of ClustalW, with 1000 bootstraps. The search for regulatory sequences of *TcSBP* was performed in the CocoaGenDB database. A region of 1500 bp upstream the UTR was identified and selected for *cis*-element analysis. The presence of the *cis*-regulatory elements in the promoter region of *TcSBP* was analyzed using the plantCARE (sphinx.rug.ac.be:8080/PlantCARE/cgi/index.html) software (Lescot et al., 2002).

2.2. Molecular modeling of *TcSBP* and docking analysis

The prediction of the three-dimensional (3-D) model of the *TcSBP* protein was obtained using the Swiss-Model server and the Automated Protein Homology-modeling, which relies on the high similarity of target-template (Arnold et al., 2006). The crystal structure of the *Sulfolobus tokodaii* SBP was used as template (Protein Data Bank code: 2ECE) to build the structural model of *TcSBP*. The stereochemical quality of the models was evaluated using the Procheck (Laskowski et al., 1993) and

Anolea programs (Melo and Feytmans, 1998). The 3-D model visualization was obtained using the PyMol (The PyMOL Molecular Graphics System, Version 1.5.0.4 Schrödinger, LLC.) and Discovery Studio 4.0. For docking analysis of *TcSBP* 3-D model (receptor) with inorganic selenium compounds (ligands), selenite and sodium selenite were search by keyword in the PubChem databases (<http://pubchem.ncbi.nlm.nih.gov>). The 2D structure of these compounds were copied in Similes and saved in PDB format using the Marvin program, and then used for molecular docking. The ligand and receptor molecules were prepared using the AutoDockTools 1.5.6 (Sanner et al., 1996). The grid definition, adjusted to active site, was set up manually according to the recommendations of the program manual (Sanner et al., 1996; Trott et al., 2010). The ligand and receptor structures were then saved in pdbqt format to be used for docking calculations. AutoDock Vina was used to perform Docking Scoring for each ligand-receptor complex (Trott et al., 2010). Before running each Docking calculation, a configuration file was generated with information about grid size and coordinates, and indicating the ligand and receptor files. The reports for each calculation were analyzed to obtain affinity energy (kCal/Mol) values for each ligand conformation in its respective complex. PyMol program was used to verify the ideal complex by considering all stereochemical aspects previously evaluated and the free-energy results. Then the best ligand i.e., that fit best in the active site, was selected.

2.3. Plant material

Plant material was obtained as previously described (Pereira Menezes et al., 2014). Seeds of *T. cacao* genotypes Catongo (susceptible to *M. perniciosa*) and TSH1188 (resistant to *M. perniciosa*) were germinated and grown at CEPLAC/CEPEC (Ilhéus, Bahia, Brazil) greenhouses. Twenty to thirty days after germination, the apical meristems of the plantlets were inoculated by the droplet method with a basidiospore suspension of *M. perniciosa* (inoculum from isolate 4145 maintained in the CEPLAC/CEPEC phytopathological *M. perniciosa* collection under number 921 of the WFCC; <http://www.wfcc.info/index.php/collections/display>). After inoculation, the plantlets were kept for 24 h at $25 \pm 2^\circ\text{C}$ and 100% humidity. Rate of disease fixation based on presence/absence of symptoms in each genotype, was evaluated 60 days after inoculation (dai); disease rate was 45% and 80% for TSH1188 and Catongo, respectively. Moreover, the presence of *M. perniciosa* in the plant material was checked by semi-quantitative RT-PCR using specific *M. perniciosa* actin primers (Pereira Menezes et al., 2014); both genotypes presented fungus incidence (data not shown) coherent with previous data obtained in the same conditions of plant culture and inoculation (Sena et al., 2014; Pereira Menezes et al., 2014). Apical meristems were harvested at 24, 48 and 72 h after inoculation (hai), and 8, 15, 30, 45, 60 and 90 dai. Non-inoculated plants (controls) were kept and harvested under the same conditions at 72 hai, 60 dai and 90 dai. For each genotype and at each harvesting time (for inoculated and non-inoculated plants), 20 samples were collected (1 sample = 1 apical meristem of 1 cacao plantlet). The 20 samples collected from one genotype at one harvesting time were pooled; thus 9 inoculated and 5 non inoculated (control) samples were immediately frozen in liquid nitrogen and stored at -80°C until use. Pooling samples before RNA extraction has the advantage of reducing the variation caused by biological replication and sample handling (Pereira Menezes et al., 2014).

2.4. Reverse transcription quantitative PCR analysis

Total RNA was extracted from macerated samples using the RNAqueous Kit® (Ambion) according to the manufacturer's instructions, with modifications as previously described (Pereira Menezes et al., 2014). The synthesis of cDNA was carried out using Revertaid First Strand cDNA Synthesis Kit according to the manufacturer's instructions (Thermo Scientific). The cDNA quantification was carried out on the GeneQuant pro UV/Vis spectrophotometer (Amersham). For the qPCR

analysis, two cacao endogenous reference genes were used: the malate dehydrogenase (MDH) and β -actin (ACT), previously identified as *T. cacao* housekeeping genes and tested in our experimental conditions (same plant material, same equipment (Pereira Menezes et al., 2014); Supplementary material 1). Specific *TcSBP* primers were also defined (Supplementary material 1). The expression analysis of *TcSBP* was performed using standard settings of the ABI PRISM 7500 and Sequence Detection System software, version 1.6.3 (Applied Biosystems). The qPCR reaction consisted of 10 ng/ μ l of cDNA, 1 μ M of each primer from reference or targets genes (Supplementary material 1) and 11 μ l of Power SYBR Green Master Mix (Applied Biosystems) in a total volume of 22 μ l. Cycling conditions were: 50 °C for 2 min then 95 °C for 10 min, followed by 40 cycles at 95 °C for 15 s, 60 °C for 30s and 60 °C for 1 min. To verify that each primer pair produced only a single PCR product, a dissociation analysis was carried out from 60 °C to 95 °C and analyzed with the Dissociation Curve 1.0 program (Applied Biosystems). The expression analysis of *TcSBP* in meristems of cacao plantlets inoculated or not with *M. perniciosa*, was obtained by RT-qPCR using 6 technical replicates. The relative expression was analyzed with the comparative Ct method ($2^{-\Delta\Delta C_t}$) using MDH and ACT as endogenous reference genes and non-inoculated plants (control) as calibrator. Statistical analysis was made using the SASM-Agri software which tested the experiments as a completely randomized design. *t*-test and *F*-test (ANOVA) were applied with a critical value of 0.01. The Scott-Knott ($P \leq 0.01$) test was employed for mean separation when *F*-values were significant.

2.5. Obtaining of the recombinant *TcSBP*

Total RNA was extracted as described above (§ 2.4) from a pool of all samples of TSH1188 *T. cacao* seedlings inoculated with the fungus *M. perniciosa* (see §2.3 and *TcSBP* expression data). The synthesis of cDNA was carried out as described above (§ 2.4). To develop a *TcSBP* cloning strategy in pET-28a(+) vector (used for heterologous expression), specific primers (F 5'-AAGACAGGGCATATGGCCGGTAACG-3' and R 5'-CGGTAAGAGTGAAGCTTCACAGCAAG-3' containing *Nde*I and *Hind*III restriction sites) were designed using the Custom Primers-OligoPerfect™ Designer (Invitrogen), OligoAnalyser 3.1 (IDT SciTools/Integrated DNA Technologies, Inc., California), and Webcutter (<http://heimanlab.com/cut2.html>) programs. The *TcSBP* amplification reaction was performed in a total volume of 25 μ l containing 1 μ l of the cDNA sample, 2.5 μ l of 10X PCR buffer, 0.75 μ l of MgCl₂ (1.5 mM), 1 μ M of each primer (0.2 mol/ μ l), 1U Recombinant Taq DNA Polymerase (Invitrogen) and ultrapure water (qsp 25 μ l). The reaction was conducted in a Veriti 96-well Thermal Cycler (Applied Biosystems) and consisted of the following steps: 4 min at 94 °C; 30 s at 94 °C; 1 min at 58 °C; 4 min at 72 °C; 7 min at 72 °C; final wait at 15 °C. The PCR product was analyzed on a 1% agarose gel stained with GelRed (Biotium). Purification of the PCR product was performed using the GFX™ PCR DNA and Gel Band Purification Kit according to the manufacturer's recommendations (GE Healthcare). The purified PCR product, as well as the pET-28a(+) vector, were digested at 37 °C for 4 h by *Nde*I and *Hind*III in a final volume reaction of 120 μ l containing 96 μ l of DNA, 12 μ l of the Tango buffer, 4.5 μ l of the each enzyme and 3 μ l of ultrapure water. After purification using the GFX™ PCR DNA and Gel

Band Purification Kit (GE Healthcare), the reactions were treated with the FastAP enzyme according to the manufacturer's recommendations (Thermo Fisher Scientific). Cloning step was performed using 90 μ l of insert, 10 μ l of pET-28a(+) vector, 10 μ l of T4-DNA ligase, 15 μ l of 10X buffer and 25 μ l of ultrapure water. Cloning reaction was used to transform *Escherichia coli* C43 strain by heat shock method (SAMBR-LOOK et al., 1989) and the transformed colonies were selected on LB medium containing kanamycin (50 μ g/ml). Transformed colonies were confirmed by PCR using the same primers and conditions as described above. For protein induction, PCR-confirmed colony was grown on LB medium at 37 °C under agitation at 180 rpm until OD_{600nm} was reached 0.6 to 1.0, then incubated with 0.4 μ mol/l of IPTG at 18 °C for 16 h under agitation, and finally centrifuged at 180 rpm. The pellet was re-suspended in 50 μ g/ml of lysozyme, kept on ice for 20 min, and then sonicated in an ice bath with 10 pulses of 10s (on), 25 pulses of 10s (off) and 70% amplitude, until breaks the pellet viscosity. The lysate material was centrifuged at 5000 rpm, 4 °C for 45 min and the supernatant was used for recombinant protein purification on TALON Superflow cobalt ion (Co²⁺) (GE Healthcare). The recombinant protein was eluted with 150 mM of imidazole and submitted to dialysis in phosphate buffer (5 mM). rTcSBP purification was checked on 15% sodium dodecyl sulfate polyacrylamide gel electrophoresis (SDS-PAGE) as previously described (Laemmli, 1970). Electrophoresis ran for 2 h at 150 V with the cube immersed in ice, and the proteins were detected on electrophoresis gel by Coomassie Blue G250 staining (Neuhoff et al., 1988). The concentration of the rTcSBP was determined by the Bradford method (Kruger and Walker, 1994) on the microplate reader ELX 800 (Biotek) using the bovine serum albumin (BSA) for the standard curve calculation.

2.6. Circular dichroism

The circular dichroism (CD) was carried out on a spectropolarimeter (model J-815, Jasco, MD) equipped with a Peltier temperature controller and a cell support with a thermostat connected to a thermostatic bath. The CD of rTcSBP was performed at a concentration of 0.355 μ g μ L⁻¹ of the protein in sodium phosphate buffer (10 mmol L⁻¹, pH 7.0). Three CD spectra (experimental replicates) of rTcSBP were measured in wavelength range of 190–240 nm at 25 °C and 95 °C. The thermal stability analysis of rTcSBP was also evaluated using unfolding (refraction denaturation from 25 to 95 °C) and refolding (variation from 95 to 25 °C) at 205 nm in sodium phosphate buffer (10 mmol L⁻¹, pH 7.0). The rTcSBP structure was also analyzed in presence of sodium selenite (1:1 M ratio) at 190–240 nm and 25 °C. The secondary α -helix and β -sheet structures were estimated using the K2D2 server (<http://cbdm-01.zdv.uni-mainz.de/~andrade/k2d2/>).

3. Results

3.1. In silico analysis of *TcSBP*

In silico analysis on CocoaGenDB revealed the presence of a unique sequence encoding *TcSBP* located on the chromosome 4 (Fig. 1). The *TcSBP* gene is 4774 bp in length, contains 7 exons and 6 introns and has

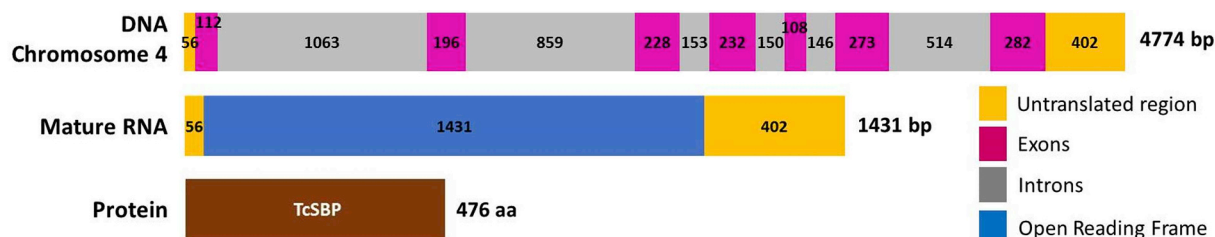


Fig. 1. Structural features of *TcSBP* sequence. Lengths of the regions are indicated at the scale.

Fig. 2. Homology modeling of TcSBP and molecular docking. **A.** Alignment of the amino acid sequence of TcSBP (XP_007034202.1) with SBPs from *Homo sapiens* (HsSBP1, AAB02395.1, UniProtKB:Q13228) and *Sulfolobus tokodaii* (StSBP, WP_010977998.1, UniProtKB:Q976Y0). Gaps introduced to get the best alignment are indicated by (-), (*) represents identical amino acids between all sequences, (.) and () represent conserved substitutions and semi-conserved substitutions, respectively. The conserved motifs DELHH, CSSC and HGD are highlighted in blue, yellow and black, respectively. Phosphorylation sites are indicated by green squares. **B.** Tridimensional structure of TcSBP obtained by homology modeling with StSBP from *Sulfolobus tokodaii* (PDB code 2ECE.pdb). **C.** Surface representation of TcSBP with the indication of the conserved motifs CSSC in pink and of putative phosphorylation sites in green. **D.** Stereo view using sticks representation with focus on the conserved CSSS motif (in pink). **E.** Docking between TcSBP and selenite at the TcSBP CSSC site. (For interpretation of the references to colour in this figure legend, the reader is referred to the Web version of this article.)

an ORF of 1431 bp (Fig. 1). *TcSBP* encodes a protein of 476 amino acids, with a MW of 52732.7 Da and a putative pI of 5.74. Twenty-one putative phosphorylation and no N-glycosylation sites were observed in the TcSBP protein sequence (Fig. 2A). TcSBP does not contain any signal peptide, and its subcellular location is unknown (data not shown). The alignment of TcSBP with SBPs from other organisms revealed high identity (> 70%) with plant species and human and allowed the identification of the CSSC, DELHH and HGD conserved region (Fig. 2A). The full-length amino acid sequences of plants and mammalian SBPs available in the databases were used to build an unrooted dendrogram (Fig. 3; Supplementary material 2). Plant and mammalian SBPs were separated and formed two distinct branches in the dendrogram (Fig. 3). *In silico* analysis of the *TcSBP* promoter region revealed the presence of several conserved *cis*-elements characteristic of different plant species (Table 1). Among these *cis*-elements, TATA-box and GA-motif related with transcription start, and with *cis*-acting in promoter and enhancer regions, respectively, were found (Table 1). Elements related to light response and circadian control (CAAT-box and Circadian, respectively) as well as elements related to response to abiotic stress or external stimuli (anaerobic induction/ARE, low-temperature response/LTR) were found. Finally, several *cis*-elements related to hormone signaling were found such as ABRE (abscisic acid responsiveness), TATC-box (gibberellin responsiveness), TCA (salicylic acid responsiveness) and TGA-box (auxin-responsive element) (Table 1).

3.2. Homology modeling of TcSBP and molecular docking of TcSBP with selenite

The modeling of the TcSBP was based in the X-ray structure of the SBP from *Sulfolobus tokodaii* (StSBP). The alignment of the amino acid sequence of TcSBP with the StSBP (Fig. 2A) presented 38% of identity, which is superior to the reliable cut-off of 25% (Schwede et al., 2003). And the structure identity between StSBP and TcSBP was 43.91% (X-ray, 2.0 Å; data not shown). The structural modeling of TcSBP revealed the presence of 7 α -helices and numerous β -strands and P-loops (Fig. 2B). The Ramachandran plots showed that 99.9% of the amino acids of the TcSBP model were located in the most favored regions (Supplementary material 3). The TcSBP showed important amino acid residues organized on domains (DELHH, HGD, CSSC/CSSA) based on its high identity (> 70%) with SBPs from other species (Fig. 2A). The tridimensional structure of TcSBP obtained by homology modeling showed that the protein contains 8 α -helices (in red, Fig. 2B) and 30 β -strands (in blue, Fig. 2B). The CSSC conserved motif of TcSBP was showed in the surface format structure (in pink, Fig. 2C) and as stick representation (in pink, Fig. 2D). Putative phosphorylation sites were present at the superficies of the protein structure; interestingly, phosphorylation sites were present in the CSSC domain of the protein (Fig. 2C). The interaction between the conserved motif CSSC of TcSBP and the selenite occurred with a setting of -1.9 kCal/mol (Fig. 2E). No interaction between TcSBP and selenate was observed (data not shown).

3.3. Production of rTcSBP and circular dichroism

The rTcSBP was expressed in *E. coli* C43, purified on affinity column, and visualized on SDS-PAGE gel (see Material and Methods). The purified rTcSBP showed molecular weight (56 kDa) coherent with the predicted one (Supplementary material 4). Circular dichroism spectra of rTcSBP in phosphate buffer pH 7.0 showed that the protein contained both α -helix and β -strand elements (Fig. 4A). The rTcSBP structure spectra showed a lower peak at ~ 205 nm, mainly at 95 °C (Fig. 4A). The rTcSBP secondary structure variation according to the temperature (unfolding and refolding) at 205 nm showed that the rTcSBP was duly folded at 25 °C and denatured from 25 °C to 95 °C (unfolding, Fig. 4B), while the refolding occurred from 95 °C to 35 °C with a fully recovery of the secondary structure at 35 °C (0% of denaturation; Fig. 4B). Circular dichroism of rTcSBP in presence and absence of sodium selenite showed that the sTcSBP interacts with selenite but that this interaction did not influence the protein structure (Fig. 4C).

3.4. Differential expression of TcSBP in resistant and susceptible cacao genotypes infected by *M. perniciosa*

The expression of the *TcSBP* gene was analyzed for each cacao genotype, i.e. TSH1188 (resistant to witches' broom disease) and Catongo (susceptible), infected or not (control) with *M. perniciosa* (Fig. 5). For both genotypes and for all the harvesting point, the PCR amplification occurred at the same and unique melting temperature for each gene showing that only the corresponding gene was amplified (Supplementary material 5). At 24 hai, *TcSBP* was significantly more expressed in inoculated susceptible variety than in the control, while its expression did not differ between inoculated resistant variety and the control plants. At 48 and 72 hai no significant difference of *TcSBP* expression between the resistant and susceptible varieties was observed, however, at 72 hai, *TcSBP* had a lower expression in the inoculated plants (whatever the genotype) than in the control plants. At 8 dai, the resistant variety showed the highest expression of *TcSBP* in relation to the other times after inoculation. At this time the susceptible variety exhibits a relative *TcSBP* expression lower than in the control plants. At 15 dai, the relative *TcSBP* expression in the resistant variety did not differ from the control, while in the susceptible variety the expression was lower than in the control plants. At 30 and 45 dai, the *TcSBP* expression was also significantly different between the varieties; *TcSBP* presented significantly higher expression in the susceptible variety. At 30 and 45 dai, in the resistant variety, *TcSBP* expression did not differ between inoculated and the control plants. At 60 and 90 dai, no significant difference in *TcSBP* expression was observed in the studied varieties.

4. Discussion

Here, we characterized a SBP gene from *T. cacao* (Figs. 1 and 2). This gene is present in the cacao genome in a unique copy located in the chromosome 4 (Fig. 1). The corresponding protein (476 amino acids;

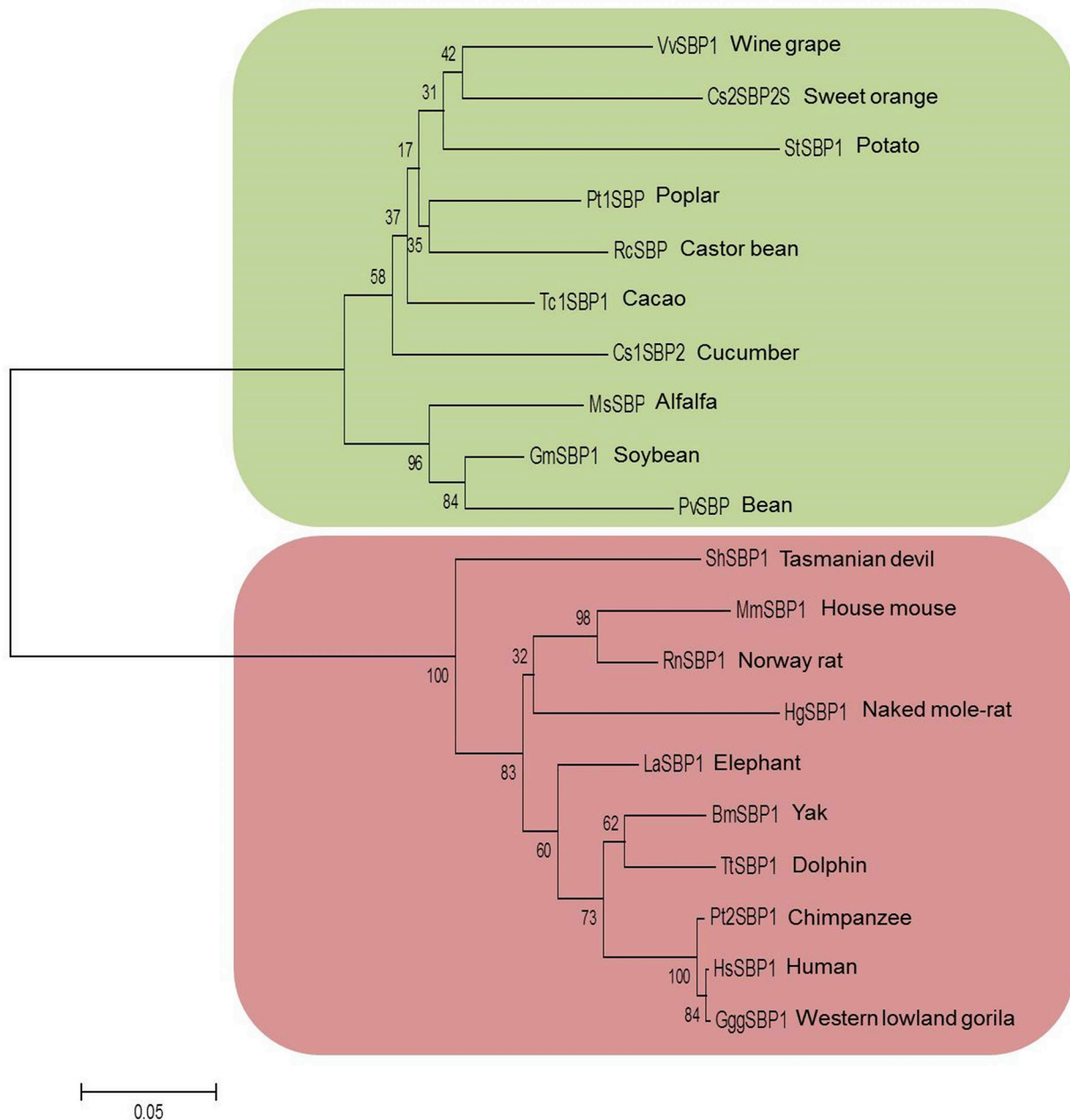


Fig. 3. Dendrogram of TcSBP and SBP from other species. The green and red boxes indicate plant and mammalian SBPs, respectively. The amino acids sequences were derived from the GenBank under the following accession numbers: VvSBP, *Vitis vinifera* (XP_002267004.1; GI:225433514); CsSBP, *Citrus sinensis* (XP_006492530.1; GI:568879129); StSBP, *Solanum tuberosum* (XP_006360921.1; GI:565390388); PtSBP, *Populus trichocarpa* (XP_006373096.1; GI:566212227); RcSBP, *Ricinus communis* (XP_002520613.1; GI:255559184); TcSBP, *Theobroma cacao* (XP_007034202.1; GI:1063488813); CsSBP, *Cucumis sativus* (XP_004138463.1; GI:449441386); MsSBP, *Medicago sativa* (AJ401228.1; CAC67501.1); GmSBP, *Glycine max* (KHN24031.1; GI:734383687); PvSBP, *Phaseolus vulgaris* (XP_007163807.1; GI:593801540); ShSBP, *Sarcophilus harrisii* (XP_003769976.1; GI: 395535935); MmSBP, *Mus musculus* (AAA40104.1; GI:200952); RnSBP, *Rattus norvegicus* (NP_001316822.1; GI: 1049480106); HgSBP, *Heterocephalus glaber* (XP_004854049.1; GI: 512984154); LaSBP, *Loxodonta africana* (XP_010587740.1; GI:731468243); BmSBP, *Bos mutus* (XP_005895013.1; GI:555965912); TtSBP, *Tursiops truncatus* (XP_019775099.1; GI:1131274601); PtSBP, *Pan troglodytes* (XP_001172033.2; GI:332810264); HsSBP, *Homo sapiens* (AAB02395.1; GI:1374792); GggSBP, *Gorilla gorilla gorilla* (XP_004026682.1; GI: 426331426). (For interpretation of the references to colour in this figure legend, the reader is referred to the Web version of this article.)

Fig. 2A) presented a secondary structure containing α -helices and β -strands (Figs. 2B and 4A) and is thermostable *in vitro* (Fig. 2A and B). Interestingly, TcSBP showed a high level of identity with the SBP from *Sulfolobus tokodaii* (Fig. 2A), which is a thermophilic archaea able to survive in high temperature environments (e.g. 70 °C) (Ohtani et al., 2004). The promoter region of TcSBP contained several *cis*-elements related to biotic stress and to hormone signaling such abscisic acid,

gibberellin, salicylic acid and auxin (Table 1). Some of these hormones are known to be highly involved in witches' broom disease development (Gesteira et al., 2007; Kilaru et al., 2007; Chaves and Gianfagna, 2006; Teixeira et al., 2014). Several genes related to plant hormone signaling were altered in cacao plants in response to *M. perniciosus* infection, such as gene involved in gibberellin response as well as auxin-responsive genes, both up-regulated in green broom (Teixeira et al.,

Table 1
Cis-elements present in the promoter region of *TcSBP* gene.

cis-elements name	Organism	Sequence	Function
ABRE	<i>Arabidopsis thaliana</i>	ACGTG	Abscisic acid responsiveness
	<i>Hordeum vulgare</i>	GCAACGTGTC	
	<i>Arabidopsis thaliana</i>	CACGTG	
ARE	<i>Zea mays</i>	AAACCA	Anaerobic induction
TATC-box	<i>Oryza sativa</i>	TATCCA	Gibberellin-responsiveness
TCA-element	<i>Nicotiana tabacum</i>	CCATCTTTT	Salicylic acid responsiveness
TGA-box	<i>Glycine max</i>	TGACGTAA	Auxin-responsive element
Circadian	<i>Lycopersicon esculentum</i>	CAAAGATATC	Circadian control
CAAT-box	<i>Brassica rapa</i>	CAAAT	Light responsive
	<i>Hordeum vulgare</i>	CAAT	
	<i>Glycine max</i>	CAATT	
GA-motif	<i>Glycine max</i>	AAGGAAGA	Cis-acting in promoter and enhancer regions
LTR	<i>Hordeum vulgare</i>	CCGAAA	Low-temperature responsiveness
TATA-box	<i>Arabidopsis thaliana</i>	TATAAA	Transcription start
	<i>Arabidopsis thaliana</i>	TATAAA	
	<i>Oryza sativa</i>	TATAAGAA	
	<i>Lycopersicon esculentum</i>	TTTTA	
	<i>Lycopersicon esculentum</i>	TTTTA	
	<i>Arabidopsis thaliana</i>	TATAA	

2014). It has been suggested that the up-regulation of auxin-responsive genes in infected cacao plants is a consequence of the biosynthesis of this hormone by *M. perniciosa* (Kilaru et al., 2007; Chaves and Gianfagna, 2006; Teixeira et al., 2014). In various plant pathogens, the production of auxin has been correlated to the reduction of the plant defenses mediated by salicylic acid, and consequently to the pathogenicity and to the biotrophic stage development (Kilaru et al., 2007; Teixeira et al., 2014). Here, we observed that the *TcSBP* gene was significantly more expressed in the susceptible variety during both the asymptomatic and the green broom stages (Fig. 4). Thus, the *TcSBP* expression may be related to its induction by hormones present at these stages as the consequence of the infection by the fungus (Fig. 4), as previously observed for SBP genes from other species (Sawada et al., 2003). In rice, the SBP expression increased rapidly in response to jasmonic acid and salicylic acid and also responded to abscisic acid and paraquat, both responsible for reactive oxygen species generation (Sawada et al., 2003).

The witches' broom disease development has been previously associated to increased H₂O₂ levels in both resistant and susceptible cacao varieties, however with distinct temporal and functional patterns (Ceita et al., 2007; Dias et al., 2011). Once produced at the beginning of the infection by the resistant variety, H₂O₂ contributes to the infection control and to plant resistance. In advanced stages of the disease in the susceptible variety, it promotes the pathogen development and the finalization of its life cycle (Dias et al., 2011). Interestingly, the *TcSBP* expression also presented distinct temporal patterns; it was higher at 8 and 15 dai in the resistant variety, and from 30 dai until the end of the disease in the susceptible variety (Fig. 4). Considering that *TcSBP* contains a CSSC conserved domain (*in silico* analysis, Fig. 2E), which is known to act as an active redox center controlling oxidation/reduction of protein *in vivo* (Sawada et al., 2003), it could be suggested that *TcSBP* gene may play a role in protecting cells from oxidative stress in swelling ramification phase in the resistant genotype, and regulating the PCD in the susceptible one during the green broom stage (Fig. 4 (Ceita et al., 2007; Dias et al., 2011)). This results could be related to the known SBP function, i.e. its capacity to inhibit the cell proliferation, and consequently its involvement in apoptosis mechanism (Zhang et al., 2013). In rice, *OsSBP* was involved in the accumulation of reactive oxygen intermediates produced by NADPH oxidase, and the observed H₂O₂ accumulation was due to the reduction of scavenging enzyme activity (Sawada et al., 2004).

Finally, the *TcSBP* protein contains multiple predicted phosphorylation sites (Fig. 2A); protein phosphorylation is a ubiquitous mechanism for the temporal and spatial regulation of proteins involved in almost every cellular process (Samuel et al., 2011). *TcSBP* contains three domains, DELHH, HGD and CSSC, highly conserved among the SBPs from other organisms (Fig. 2A); the CSSC domain contained predicted phosphorylation sites (Fig. 2C). It has been suggested that the characteristic CSSC motif has a strong affinity for selenium and heavy metals (Wu et al., 2010). In *T. cacao*, we observed that the conserved domain CSSC was able to bind, *in silico*, the selenite (Fig. 2E). The binding of rTcSBP with the selenite was confirmed *in vitro* by circular dichroism, showing that this interaction did not modify the protein structure (Fig. 4C). Some phosphorylation sites (the stable ones) are known to be important for the regulatory function of the protein (Ardito et al., 2017) and, here, it may be suggested that the phosphorylation at the CSSC domain may be related to the binding with selenite, as well as to the protein function as regulator of oxidation/reduction during the plant-pathogen interaction. Moreover, the conserved domain CSSC potentially may be a binding site for other metals as observed in other organisms (Wu et al., 2010). This could be interesting considering the concerns about high concentrations of heavy metals (e.g. Pb, Cd, Cu) found in beans of cacao as well as in its products (including chocolate). Contamination of cacao is attributed to the increasing use of phosphate fertilizers but also to several kinds of industrial processes close to the cacao production areas (Arévalo-Gardini et al., 2017).

5. Conclusion

Here we showed the first *in silico* and *in vitro* analysis of the SBP from cacao. The rTcSBP is a thermostable protein able to bind *in silico* and *in vitro* the selenite and potentially may be able to bind heavy metals. *TcSBP* is differentially expressed in resistant vs susceptible cacao varieties inoculated by *M. perniciosa* and its expression is probably due to hormone induction (e.g. indole acetic acid, salicylic acid, gibberellins) via *cis*-regulating elements present in its promoter (e.g. TATC-box, TCA, TGA-box). The presence of the CSSC conserved domain in *TcSBP* structure suggested that *TcSBP* acted by altering oxidation/reduction of proteins during H₂O₂ production and PCD in the final stages of the witches' broom disease. For these reasons, the *TcSBP* appeared to be a good candidate for biotechnological applications aiming control of biotic (e.g. pathogens) and abiotic (e.g. heavy metals) stresses.

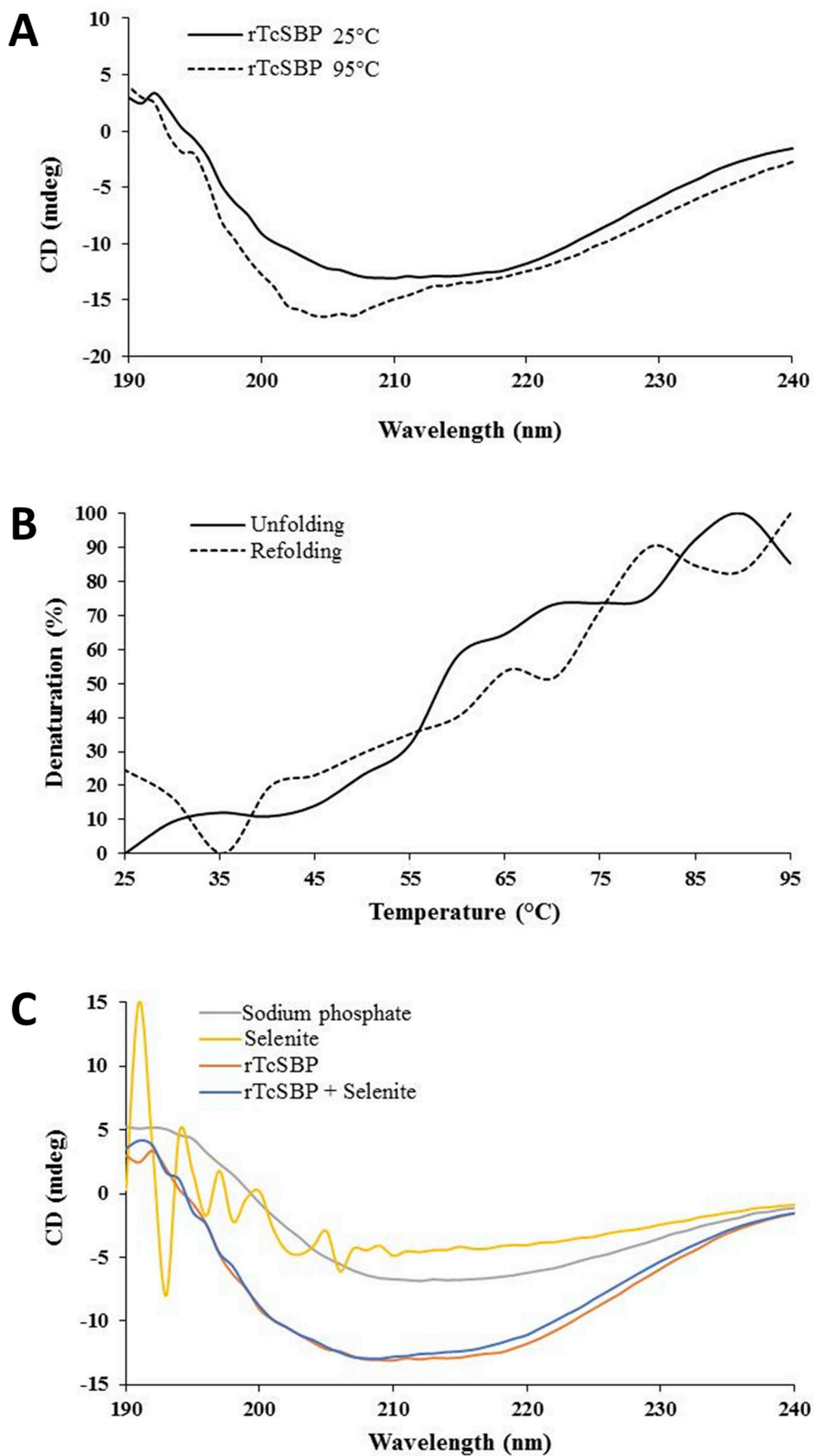


Fig. 4. Circular dichroism analysis of rTcSBP. **A.** Spectra of the rTcSBP secondary structure at 190–240 nm. Black and dashed lines corresponded to the rTcSBP structure at 25 °C and 95 °C, respectively. **B.** Unfolding (black line) and refolding (dashed line) of rTcSBP in phosphate buffer (pH 7.0) at 205 nm. **C.** Secondary structure of rTcSBP in presence of sodium selenite at 25 °C. The grey line corresponds to sodium phosphate buffer scan, yellow line to sodium selenite scan, orange line to rTcSBP scan, and blue line to rTcSBP with sodium selenite scan (1:1 ratio). (For interpretation of the references to colour in this figure legend, the reader is referred to the Web version of this article.)

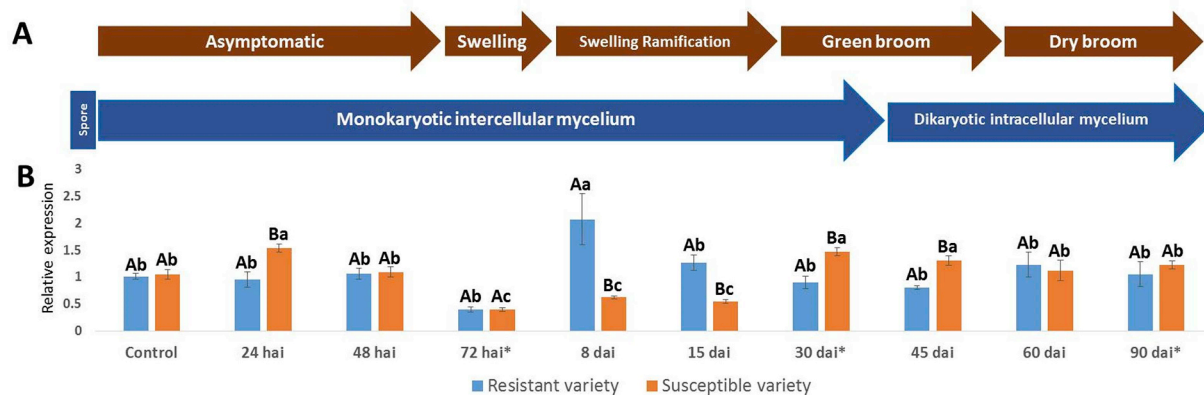


Fig. 5. Relative expression of *TcSBP* in cacao meristems inoculated or not (control) with *M. perniciosa*. **A.** Representation of the plant symptoms and fungus phase during the infection time course in Catongo genotype. **B.** Relative expression observed in resistant (TSH1188) and susceptible (Catongo) varieties. Different letters indicate significant statistical difference between samples by the Scott-Knott test ($p \leq 0.01$). *t*-test were applied with a critical value of 0.01: upper case letters correspond to statistics between each of the genes on different harvesting times for each genotype while lower case letters correspond to statistics between the three genes for each harvesting time. hai: hours after inoculation; dai: days after inoculation. (*) indicates the times that were harvested also in the non-inoculated (control) plants.

Conflicts of interest

No conflicts of interest to declare.

Authors' contribution

AMMA was responsible for the execution of all the experimental steps; AMMA, SPM, BSA and FM analyzed and discussed the data; AMMA and FM wrote the manuscript; SPM and EML gave support in qPCR experiment; BSA gave support in modeling and docking analyses; KPG was responsible for plant material production and inoculation with *M. perniciosa*; MMF and CPP supported the circular dichroism analysis; FM and BSA were responsible for the conception and design of the experiments; FM was responsible for the financial support of the research and for the advising of AMMA, EML and SPM.

Acknowledgements

The work of AMMA was supported by the Fundação de Amparo à Pesquisa do Estado da Bahia (FAPESB). The work of SPM, EML and MMF was supported by the Coordenação de Aperfeiçoamento de Pessoal de Nível Superior (CAPES). FM, KPG and CPP were supported by a Productivity grant from Conselho Nacional de Desenvolvimento Científico e Tecnológico (CNPq). This research was supported by the FAPESB project (DTE0038/2013) coordinated by FM. The authors thank Francisca Feitosa Jucá (UESC/Ceplac) and Louise Araújo Sousa (Ceplac) for technical help in plant inoculation experiments, Dr. Gesilvado Santos (UESB) for advices and discussion about SBP role. This research was made in the frame of the International Consortium in Advanced Biology (CIBA).

Abbreviations

ACT	actin
dai	days after inoculation
hai	hour after inoculation
pI	isoelectric point
MDH	malate dehydrogenase
MW	molecular weight
ORF	open reading frame
PCD	programmed cell death
SBP	selenium-binding protein
Se	selenium
UTR	untranslated regions

Appendix A. Supplementary data

Supplementary data to this article can be found online at <https://doi.org/10.1016/j.plaphy.2019.08.005>.

References

- Agalou, A., Roussis, A., Spaink, H.P., 2005. The Arabidopsis selenium-binding protein confers tolerance to toxic levels of selenium. *Funct. Plant Biol.* 32, 881–890.
- Altschul, S.F., Madden, T.L., Schaffer, A.A., Zhang, J., Zhang, Z., Miller, W., Lipman, D.J., 1997. Gapped BLAST and PSI-BLAST: a new generation of protein database search programs. *Nucleic Acids Res.* 25, 3389–3402.
- Ansong, E., Yang, W., Diamond, A.M., 2014. Molecular cross-talk between members of distinct families of selenium containing proteins. *Mol. Nutr. Food Res.* 58, 117–123.
- Ardito, F., Giuliani, M., Perrone, D., Troiano, G., Lo Muzio, L., 2017. The crucial role of protein phosphorylation in cell signaling and its use as targeted therapy (Review). *Int. J. Mol. Med.* 40, 271–280.
- Arévalo-Gardini, E., Arévalo-Hernández, C.O., Baligar, V.C., He, Z.L., 2017. Heavy metal accumulation in leaves and beans of cacao (*Theobroma cacao* L.) in major cacao growing regions in Peru. *Sci. Total Environ.* 605–606, 792–800.
- Arnold, K., Bordoli, L., Kopp, J., Schwede, T., 2006. The SWISS-MODEL workspace: a web-based environment for protein structure homology modelling. *Bioinformatics* 22, 195–201.
- Blom, N., Gammeltoft, S., Brunak, S., 1999. Sequence and structure-based prediction of eukaryotic protein phosphorylation sites. *J. Mol. Biol.* 294, 1351–1362.
- Ceita, G.O., Macedo, J., Santos, T., Alemanno, L., Gesteira, A.S., Micheli, F., Mariano, A., Gramacho, K., Silva, D.C., Meinhardt, L., 2007. Involvement of calcium oxalate degradation during programmed cell death in *Theobroma cacao* tissues triggered by the hemibiotrophic fungus *Moniliophthora perniciosa*. *Plant Sci.* 173, 106–117.
- Chaves, F.C., Gianfagna, T.J., 2006. Necrotrophic phase of *Moniliophthora perniciosa* causes salicylic acid accumulation in infected stems of cacao. *Physiol. Mol. Plant Pathol.* 69, 104–108.
- Dias, C.V., Mendes, J.S., dos Santos, A.C., Pirovani, C.P., da Silva Gesteira, A., Micheli, F., Gramacho, K.P., Hammerstone, J., Mazzafera, P., de Mattos Cascardo, J.C., 2011. Hydrogen peroxide formation in cacao tissues infected by the hemibiotrophic fungus *Moniliophthora perniciosa*. *Plant Physiol. Biochem.* 49, 917–922.
- Emanuelsson, O., Brunak, S., von Heijne, G., Nielsen, H., 2007. Locating proteins in the cell using TargetP, SignalP and related tools. *Nat. Protoc.* 2, 953–971.
- Evans, H.C., 2007. Cacao diseases—the trilogy revisited. *Phytopathology* 97, 1640–1643.
- Gasteiger, E., Hoogland, C., Gattiker, A., Duvaud, S., Wilkins, M.R., Appel, R.D., Bairoch, A., 2005. Protein identification and analysis tools on the ExPASy server. In: Walker, J.M. (Ed.), *The Proteomics Protocols Handbook*. Humana Press, pp. 571–607.
- Gesteira, A.S., Micheli, F., Carels, N., Da Silva, A., Gramacho, K., Schuster, I., Macedo, J., Pereira, G., Cascardo, J., 2007. Comparative analysis of expressed genes from cacao meristems infected by *Moniliophthora perniciosa*. *Ann. Bot.* 100, 129–140.
- Kilaru, A., Bailey, B.A., Hasenstein, K.H., 2007. *Moniliophthora perniciosa* produces hormones and alters endogenous auxin and salicylic acid in infected cocoa leaves. *FEMS (Fed. Eur. Microbiol. Soc.) Microbiol. Lett.* 274, 238–244.
- Kruger, N.J., 1994. The Bradford method for protein quantitation. In: Walker, J.M. (Ed.), *Basic Protein and Peptide Protocols*. Humana Press, Totowa, NJ, pp. 9–15.
- Laemmli, U.K., 1970. Cleavage of structural proteins during the assembly of the head of bacteriophage T4. *Nature* 227, 680–685.
- Larkin, M.A., Blackshields, G., Brown, N.P., Chenna, R., McGettigan, P.A., McWilliam, H., Valentin, F., Wallace, I.M., Wilm, A., Lopez, R., Thompson, J.D., Gibson, T.J., Higgins, D.G., 2007. Clustal W and clustal X version 2.0. *Bioinformatics* 23,

- 2947–2948.
- Laskowski, R.A., MacArthur, M.W., Moss, D.S., Thornton, J.M., 1993. PROCHECK: a program to check the stereochemical quality of protein structures. *J. Appl. Crystallogr.* 26, 283–291.
- Lescot, M., Déhais, P., Thijs, G., Marchal, K., Moreau, Y., Van de Peer, Y., Rouzé, P., Rombauts, S., 2002. PlantCARE, a database of plant cis-acting regulatory elements and a portal to tools for in silico analysis of promoter sequences. *Nucleic Acids Res.* 30, 325–327.
- Melo, F., Feytmans, E., 1998. Assessing protein structures with a non-local atomic interaction energy. *J. Mol. Biol.* 277, 1141–1152.
- Nakai, K., Horton, P., 1999. PSORT: a program for detecting sorting signals in proteins and predicting their subcellular localization. *Trends Biochem. Sci.* 24, 34–35.
- Neuhoff, V., Arold, N., Taube, D., Ehrhardt, W., 1988. Improved staining of proteins in polyacrylamide gels including isoelectric focusing gels with clear background at nanogram sensitivity using Coomassie Brilliant Blue G-250 and R-250. *Electrophoresis* 9, 255–262.
- Ohtani, N., Yanagawa, H., Tomita, M., Itaya, M., 2004. Cleavage of double-stranded RNA by RNase HI from a thermoacidophilic archaeon, *Sulfolobus tokodaii* 7. *Nucleic Acids Res.* 32, 5809–5819.
- Pereira Menezes, S., de Andrade Silva, E., Matos Lima, E., Oliveira de Sousa, A., Silva Andrade, B., Santos Lima Lemos, L., Peres Gramacho, K., da Silva Gesteira, A., Pirovani, C., Micheli, F., 2014. The pathogenesis-related protein PR-4b from *Theobroma cacao* presents RNase activity, Ca²⁺ and Mg²⁺ dependent-DNase activity and antifungal action on *Moniliophthora perniciosa*. *BMC Plant Biol.* 14, 1–17.
- Petersen, T.N., Brunak, S., von Heijne, G., Nielsen, H., 2011. SignalP 4.0: discriminating signal peptides from transmembrane regions. *Nat. Methods* 8, 785–786.
- SAMBROOK, J., FRITSCH, E.F., MANIATIS, E.F.T., 1989. *Molecular Cloning - a Laboratory Manual*. Cold Spring Harbor, New York.
- Pearlman, Samuel.M., Serber, Z., Ferrell Jr., James E., 2011. A mechanism for the evolution of phosphorylation sites. *Cell* 147, 934–946.
- Sanner, M., Olson, A.J., Spohner, J.C., 1996. Reduced surface: an efficient way to compute molecular surfaces. *Biopolymers* 38, 305–320.
- Sawada, K., Tokuda, L., Shinmyo, A., 2003. Characterization of the rice blast fungal elicitor-responsive gene OsSBP encoding a homolog to the mammalian selenium-binding proteins. *Plant Biotechnol.* 20, 177–181.
- Sawada, K., Hasegawa, M., Tokuda, L., Kameyama, J., Kodama, O., Kohchi, T., Yoshida, K., Shinmyo, A., 2004. Enhanced resistance to blast fungus and bacterial blight in transgenic rice constitutively expressing OsSBP, a rice homologue of mammalian selenium-binding proteins. *Biosci. Biotech. Biochem.* 68, 873–880.
- Schwede, T., Kopp, J.r., Guex, N., Peitsch, M.C., 2003. SWISS-MODEL: an automated protein homology-modeling server. *Nucleic Acids Res.* 31, 3381–3385.
- Sena, K., Alemanno, L., Gramacho, K.P., 2014. The Infection Process of *Moniliophthora perniciosa* in Cacao, *Plant Pathology*. pp. 1272–1281.
- Tamura, K., Stecher, G., Peterson, D., Filipksi, A., Kumar, S., 2013. MEGA6: molecular evolutionary genetics analysis version 6.0. *Mol. Biol. Evol.* 30, 2725–2729.
- Teixeira, P.J.P.L., Thomazella, D.P.d.T., Reis, O., do Prado, P.F.V., do Rio, M.C.S., Fiorin, G.L., José, J., Costa, G.G.L., Negri, V.A., Mondego, J.M.C., Mieczkowski, P., Pereira, G.A.G., 2014. High-resolution transcript profiling of the atypical biotrophic interaction between *Theobroma cacao* and the fungal pathogen *Moniliophthora perniciosa*. *The Plant Cell* 26, 4245–4269.
- Trott, O., Olson, A.J., Vina, A.D., 2010. Improving the speed and accuracy of docking with a new scoring function, efficient optimization and multithreading. *J. Comput. Chem.* 31, 455–461.
- Valassakis, C., Livanos, P., Minopetrou, M., Haralampidis, K., Roussis, A., 2018. Promoter analysis and functional implications of the selenium binding protein (SBP) gene family in *Arabidopsis thaliana*. *J. Plant Physiol.* 224–225, 19–29.
- Wood, G.A.R., Lass, R.A., 1985. In: *Cocoa*, fourth ed. ed. Blackwell Science Ltd..
- Wu, C.-L., Zhang, W.-B., Mai, K.-S., Liang, X.-F., Xu, W., Wang, J., Ma, H.-M., 2010. Molecular cloning, characterization and mRNA expression of selenium-binding protein in abalone (*Haliotis discus hannai* Ino): response to dietary selenium, iron and zinc. *Fish Shellfish Immunol.* 29, 117–125.
- Zhang, S., Li, F., Younes, M., Liu, H., Chen, C., Yao, Q., 2013. Reduced selenium-binding protein 1 in breast cancer correlates with poor survival and resistance to the anti-proliferative effects of selenium. *PLoS One* 8, e63702.